

Using Fourier Transform and Model Based Filters to Measure Time-Varying Harmonics

Jeroen Van den Keybus, *Member, IEEE*, Johan Driesen, *Member, IEEE*
and Ronnie Belmans, *Senior Member, IEEE*

Abstract — Power quality problems have become an important issue in electrical power systems design and operation. Therefore, methods to identify and quantify these problems are receiving increased attention. A good deal of those methods rely on the time-varying phasor description of power system currents and voltages. This paper is an attempt to summarize two established processing techniques to obtain these quantities based on a time sampled data stream. The first class of methods is based on the Fourier transform, whereas the second is model based. Finally, references to new processing techniques are given.

Index Terms — power system harmonics, Fourier transform, Kalman filter, wavelet transform

I. INTRODUCTION

THIS paper contains a brief description of measurement techniques used to obtain the harmonic content of current or voltage measurements. First, the front-end signal chain is outlined, the output of which is assumed to be a digital data stream. Then, three methods are discussed to produce the harmonic signal content based on this digital, sampled data stream.

The first method is the well-known Fast Fourier Transform (FFT). The second one is a model-based technique. These two methods are essentially Finite Impulse Response (FIR) and Infinite Impulse Response (IIR) filters, an important property to consider when applying them to non-stationary signals (i.e. signals in which the harmonic content varies in time). Wavelet analysis is briefly mentioned as a third method, indicating the existence and potential of more advanced analysis techniques.

II. CURRENT AND VOLTAGE ACQUISITION

A. Measurement Method

The measurement of both current and voltage is commonly performed in four steps:

1. *Scaling*. This step converts the physical voltage or current to a value that is small enough to communicate through signal cables, but not too small to avoid noise pickup.

Scaling devices include current and voltage transformers and capacitive dividers, with a precision of 0.1 to 5 % at 50 or 60 Hz. Typically, the analog output rms value of a scaling operation lies in the range of 60 to 600 V for the voltage and 0.1 to 5 A for the current measurement.

2. *Isolation*. Galvanic isolation is mandatory for safety reasons and is often combined with the scaling operation. The construction of a precision isolation barrier for analog signals is not easy. As an alternative, the barrier may be inserted after step 4, when the signal is digital. The entire measurement system is then allowed to float at the potential of the power system.
3. *Conditioning*. Analog to digital converters (ADCs) require a voltage input signal. Precision shunt resistances convert current input signals to a small voltage, which is subsequently amplified. A voltage input signal, on the other hand, is further scaled down and buffered. Conditioning also includes filtering to prevent aliasing errors.
4. *Analog to digital conversion*. The ADC is a single component converting the input signal to a digital value. Monolithic ADCs with resolutions of up to 24 bits are currently available and often reported, although 20 bits is rather a realistic limiting value if sampling rates of more than 100 Hz are desired.

Two remarks must be made to this overview. First, the isolation barrier is not only advantageous for protection reasons. It also avoids ground loops and interference, especially if the power system contains noise at high frequencies, which is often the case if switching converters are present nearby. Some researchers [1] also decided on using fully floating measurement heads after being plagued by interference.

Secondly, the overview applies to sampling ADCs, which take a sample of their input, convert it somehow and deliver the output value in one cycle. Other types exist, such as delta-sigma and pipelined ADCs. The pipelined ADC uses several conversion stages in series, leading to sample rates of more than 125 MSa/s at 14 bit, but with e.g. a 16.5 sample delay [2]. The delta-sigma ADC is basically a single bit converter, which produces a high-frequency bit stream that needs to be filtered digitally. As a result, these converters have a reduced input filtering requirement, facilitating the design of the conditioning electronics. They are excellent for 50 or 60 Hz

J. Van den Keybus, J. Driesen, and R. Belmans are with the Department of Electrical Engineering, research group ELECTA Katholieke Universiteit Leuven, B-3001 Leuven, Belgium (e-mail: vdkeybus@esat.kuleuven.ac.be, <http://www.esat.kuleuven.ac.be/electa>).

measurements, which explains why many electronic wattmeter chip sets are based on them.

B. Measurement of phasor quantities – Time dependency of phasors

Strictly speaking, the specification of the harmonic signal content (also known as phasor description) also implies that the signal is periodic. Because of this requirement, one fundamental frequency period is sufficient to fully determine all phasors. Excluding noise, the analysis of another equally sized time frame would invariably lead to the same result.

In practice, signals are seldom strictly periodic (e.g. any physical system must be powered up at some point in time) and as such frequency domain analysis is theoretically impossible. On the other hand, prolonged periods exist in which, apart from noise, signals are perfectly periodic, and in which a frequency domain analysis is actually a sensible thing to carry out. Thus, the phasors determined from experiments performed at two distinct points in time might differ, indicating a time dependency of the phasors obtained in such way.

The next sections deal with techniques to determine voltage or current phasors based on a frame of consecutive current and voltage samples. First, the well-known Fourier Transform (FT) is highlighted. Next, model based techniques are described and compared to the FT. Finally, reference is made to wavelet-based techniques.

III. FOURIER TRANSFORM

A. Introduction

The Fourier transform is widely used and covered by many textbooks and other publications. Therefore, the discussion of this integral transform is kept short and the reader must refer to e.g. [3] for an in-depth treatment.

The continuous time Fourier transform provides the full frequency domain description of any arbitrary signal, but is impossible to apply in practical sampled data systems. Its discrete time counterpart, the Discrete Fourier Transform (DFT), is given by:

$$\underline{c}_n = \sum_{k=0}^{N-1} y_k e^{-2\pi jnk/N} \quad (1)$$

It is very popular due to its computationally efficient implementation, the Fast Fourier Transform (FFT). Furthermore, if the N samples of y_k exactly cover an integer number of grid cycles, it readily provides the phasors.

A few assumptions are intrinsically made when applying the DFT for power phasor measurements:

1. the signal is strictly periodic;
2. the sampling frequency is an integer multiple of the fundamental grid angular frequency ω_G ;
3. the sample frequency is at least twice the highest frequency in the signal to be analyzed;

4. each frequency in the signal is an integer multiple of the fundamental frequency.

Additionally, when using an FFT it is advantageous to have a number of samples that is an integer power of two.

When the above assumptions are satisfied, the results of the DFT are accurate, but if they are not, generally, three problems are encountered [4]: aliasing, leakage and the picket-fence effect.

1. *Aliasing* – Aliasing originates from the presence of frequencies in the signal above $f_S/2$, the Nyquist frequency. Although an anti-aliasing filter may be present in the data acquisition system, special attention must be paid to the noise introduced in the measurement system after this filter.
2. *Leakage* – The DFT must be performed on a finite series of signal samples. Leakage is caused by truncation of the (theoretically) infinite measurement series y_k . It is unavoidable and can be mitigated by the use of window functions. If the signal is periodic and an integer number of periods is used for analysis, there is no leakage.
3. *Picket-fence effect* – Picket fencing occurs when the signal contains a frequency that is not an integer multiple of the fundamental frequency (interharmonic), increasing the Fourier coefficients of neighboring frequencies. Again, if the signal is periodic and well synchronized to the signal samples, no interharmonics exist.

B. Synchronization errors

If the sampling frequency f_S and the grid fundamental frequency are not properly synchronized, the leakage and the picket fence effect occur simultaneously.

It can be shown [5] that the phasor value of the k^{th} harmonic has an error proportional to the synchronization frequency error, and inversely proportional to the order of the harmonic. Phasors that should be zero deviate in roughly the same manner, but are also proportional to f_S . Therefore, if the measurement is badly synchronized, the presence of a strong harmonic impedes the accurate assessment of other small harmonics.

In islanding grids, the accuracy of the grid frequency may very well be in the order of 1 %. In this case, synchronization using e.g. a Phase Locked Loop (PLL) is indispensable.

The DFT may also be used to analyze more than one period of the fundamental frequency. The leakage effect is less dominant in this case. This method is used in the IEC 61000-4-7 standard, at the expense of a longer observation interval.

C. Filter properties and transient response

Observing (1), the DFT can be considered a Finite Impulse Response (FIR) filter, having the following properties.

1. If the filter length is N , any input before the N last samples no longer contributes to the output.

2. A FIR filter never becomes unstable.

The transition from a periodic signal with amplitude A_n and phase ϕ_n to another periodic signal with amplitude A_n' and phase ϕ_n' causes the signal temporarily not to meet the periodicity requirement and due to property 1, one must wait at least N cycles before the phasor calculation of the signal becomes valid again.

D. Computational effort

The computational effort to compute the $N/2$ Fourier coefficients from N samples is proportional to $N \log_2(N)$. If the calculation is done in sliding mode, i.e. the FFT is repeatedly applied to a frame of N elements consisting of the last $N - 1$ shifted elements of the previous frame and a single new element, $N^2 \log_2(N)$ calculations are needed.

IV. MODEL BASED TECHNIQUES

A. Introduction

Model based harmonic estimation is quite different from the Fourier transform approach. The technique is based on a mathematical model of the system to be analyzed and uses voltage or current measurements to correct the state of the model. At any time, phasors can be derived from the model state, which is updated every time a measurement becomes available. This is a clear advantage over the DFT that processes entire frames of data and cannot provide in-between data.

B. Linear discrete time Kalman filter

The discrete Kalman filter is as much an algorithm as it is a filter. For completeness, the main equations are repeated here, but the reader must refer to the many existing, excellent handbooks (e.g. [6]) covering Kalman filtering in depth.

System modeling is done using the state variable approach, i.e. the system is modeled in the discrete time domain:

$$\begin{aligned} \mathbf{x}_{k+1} &= \mathbf{A}\mathbf{x}_k + \mathbf{B}\mathbf{u}_k \\ \mathbf{y}_k &= \mathbf{C}\mathbf{x}_k + \mathbf{D}\mathbf{u}_k \end{aligned} \quad (2)$$

\mathbf{x}_k is the state vector, \mathbf{y}_k is the output vector and \mathbf{u}_k is the input vector of the system at time point k . The \mathbf{A} and \mathbf{B} matrices entirely describe the system's behavior.

Suppose the system to be observed can be described in discrete state space by:

$$\mathbf{x}_{k+1} = \Phi_k \mathbf{x}_k + \mathbf{w}_k \quad (3)$$

It is assumed that a number of process states (elements of \mathbf{x}_k) are measured by:

$$\mathbf{y}_k = \mathbf{H}_k \mathbf{x}_k + \mathbf{v}_k \quad (4)$$

Note that both Φ_k and \mathbf{H}_k can be time-dependent. In these

equations, \mathbf{w}_k and \mathbf{v}_k are white noise sequences with a known covariance structure. They represent the inability of the model to track the observed system on one hand and the measurement errors on the other. The stochastic properties of \mathbf{v}_k and \mathbf{w}_k can be mathematically described by:

$$\begin{aligned} E[\mathbf{w}_k \mathbf{w}_i^T] &= \mathbf{Q}_k \quad (i = k), \quad 0 \quad (i \neq k) \\ E[\mathbf{v}_k \mathbf{v}_i^T] &= \mathbf{R}_k \quad (i = k), \quad 0 \quad (i \neq k) \\ E[\mathbf{v}_k \mathbf{w}_i^T] &= 0 \end{aligned} \quad (5)$$

in which $E[\]$ represents the expectancy operator. In other words, the noises described by the elements of \mathbf{v} and \mathbf{w} are white. Next, the estimation error is defined as:

$$\mathbf{e}_k^- = \mathbf{x}_k - \hat{\mathbf{x}}_k^- \quad (6)$$

with the associated covariance matrix:

$$\mathbf{P}_k^- = E[\mathbf{e}_k^- \mathbf{e}_k^{-T}] \quad (7)$$

\mathbf{x}_k denotes the real, 'correct' state which is immeasurable, and $\hat{\mathbf{x}}_k^-$ is the estimate of \mathbf{x}_k . The circumflex ' $\hat{\ }$ ' indicates that the variable is an estimation and ' $-$ ' means that the estimation is an a priori one, i.e. based on all previous information but the last measurement, \mathbf{z}_k . The a posteriori estimate is obtained, based on the a priori estimate and the difference between the new measurement and its expected value:

$$\hat{\mathbf{x}}_k = \hat{\mathbf{x}}_k^- + \mathbf{K}_k (\mathbf{z}_k - \mathbf{H}_k \hat{\mathbf{x}}_k^-) \quad (8)$$

\mathbf{K}_k is the Kalman gain for time instant k . It shows that blending occurs between the previous estimate and the measurement's deviation from the expected one, which indicates a state estimation mismatch. The calculation of the successive Kalman gains \mathbf{K}_k can be conveniently summarized in a loop, Fig. 1, clearly demonstrating the algorithmic nature of the Kalman filter [6].

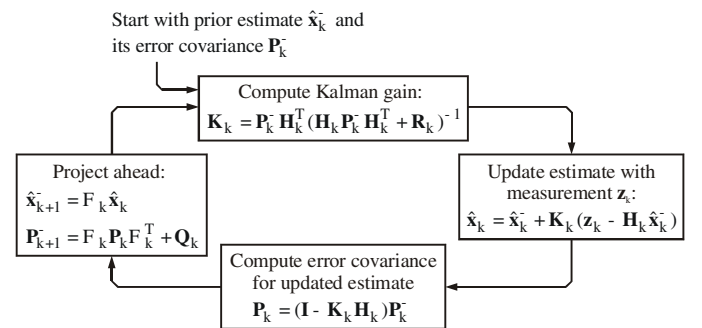


Fig. 1. Kalman filter loop [6].

C. Time invariant linear discrete Kalman filter

In many cases, Φ_k , \mathbf{H}_k , \mathbf{Q}_k and \mathbf{R}_k all are time invariant and therefore, do not depend on k . In that case, \mathbf{K}_k and \mathbf{P}_k calculated in the algorithm shown in Fig. 1, converge to a time invariant gain \mathbf{K} and an associated covariance matrix \mathbf{P} .

The calculation of \mathbf{K} and \mathbf{P} can be done offline (e.g. using

the MATLAB `kalman` command) and the use of the estimator then reduces to the evaluation of equation (8), with a minimum of computational effort.

D. State variable description of a sinusoidal signal

There are two methods to represent a sinusoidally varying signal in the state space [7][8]. The *first method (Model 1)* uses a harmonic oscillator.

$$\begin{aligned} \begin{bmatrix} x_{\text{Re}} \\ x_{\text{Im}} \end{bmatrix}_{k+1} &= \mathbf{x}_{k+1} \\ &= \mathbf{A}_{\text{OSC1}} \mathbf{x}_k = \begin{bmatrix} \cos(\omega\Delta t) & \sin(\omega\Delta t) \\ -\sin(\omega\Delta t) & \cos(\omega\Delta t) \end{bmatrix} \begin{bmatrix} x_{\text{Re}} \\ x_{\text{Im}} \end{bmatrix}_k \end{aligned} \quad (9)$$

Note that the state transition matrix \mathbf{A}_{OSC1} is constant. \mathbf{x} is a vector containing the real (in-phase) and imaginary (quadrature) part of the harmonic oscillator. ω is the natural pulsation and Δt represents the model's sample time.

\mathbf{A}_{OSC1} can also be considered a transformation matrix, rotating the vector \mathbf{x} over an angle $\varphi = \omega\Delta t$ in every time step whilst preserving its amplitude. The output of the system, y_k , is given by the in-phase component, thus:

$$\begin{aligned} \mathbf{C}_{\text{OSC1}} &= \begin{bmatrix} 1 & 0 \end{bmatrix} \\ \mathbf{D}_{\text{OSC1}} &= 0 \end{aligned} \quad (10)$$

The *second method (Model 2)* is also mentioned in [7] and uses a state vector representing a phasor instead of the actual voltages, which, ideally, does not change. Therefore:

$$\mathbf{x}_{k+1} = \mathbf{A}_{\text{OSC2}} \mathbf{x}_k = \begin{bmatrix} 1 & 0 \\ 0 & 1 \end{bmatrix} \mathbf{x}_k \quad (11)$$

The measurement equation may be expressed as:

$$\begin{aligned} \mathbf{C}_{\text{OSC2}} &= \begin{bmatrix} \sin(\omega t_k) & \cos(\omega t_k) \end{bmatrix} \\ \mathbf{D}_{\text{OSC2}} &= 0 \end{aligned} \quad (12)$$

In this case, \mathbf{C}_{OSC2} is no longer constant in time. Both systems have no input ($\mathbf{B}_{\text{OSC1}} = \mathbf{B}_{\text{OSC2}} = 0$). Once started with an initial state vector \mathbf{x}_0 , they output the same sine waveform forever. The associated states are uncontrollable, but observable.

E. Grid voltage modeling

In what follows, the model based grid voltage estimation is highlighted. The grid voltage is not stationary and contains noise of various origins. The measurement taken to improve the grid voltage estimation may also contain noise.

To some extent, the grid voltage non-stationarity and noise can be modeled as a single white noise source $\mathbf{w}(t)$. A second, white noise source $v(t)$ represents the measurement errors. Including these noises, the grid voltage model is:

$$\begin{aligned} \mathbf{x}_{k+1} &= \mathbf{A} \mathbf{x}_k + \mathbf{w}_k \\ y &= \mathbf{C} \mathbf{x}_k + v_k \end{aligned} \quad (13)$$

in which $v_k = v(k\Delta t)$ and $\mathbf{w}_k = \mathbf{w}(k\Delta t)$ are the sampled data versions of $v(t)$ and $\mathbf{w}(t)$ and the \mathbf{A} and \mathbf{C} matrices must be replaced by \mathbf{A}_{OSC1} and \mathbf{C}_{OSC1} , or \mathbf{A}_{OSC2} and \mathbf{C}_{OSC2} , depending on which grid modeling technique is used. Also note that \mathbf{w}_k is a vector containing two independent white noise sources.

In the form of (2) and provided that \mathbf{Q} and \mathbf{R} are available, the model can be processed by the Kalman filter. Note that \mathbf{C}_{OSC2} in Model 2 is time-dependent and the algorithm of Fig.1, must be executed for every time step to obtain the – also time-dependent – Kalman gain \mathbf{K}_k .

F. Transient response

The dynamic behavior of the first model based grid voltage estimator (Model 1) is studied by observing the response to a state mismatch $\mathbf{e}_k = \mathbf{x}_k - \hat{\mathbf{x}}_k$. Fig. 2, shows the data flow schematically. In this section, for notational convenience, \mathbf{A} and \mathbf{C} are used to represent \mathbf{A}_{OSC1} and \mathbf{C}_{OSC1} , respectively.

Under the assumption that the model is perfect, i.e. $\mathbf{A} = \mathbf{A}'$ and $\mathbf{C} = \mathbf{C}'$, the state estimation error \mathbf{e}_k can be rewritten as:

$$\begin{aligned} \mathbf{e}_{k+1} &= \mathbf{x}_{k+1} - \hat{\mathbf{x}}_{k+1} \\ &= \mathbf{A}' \mathbf{x}_k - \mathbf{A} \hat{\mathbf{x}}_k - \mathbf{L}(\mathbf{C}' \mathbf{x}_k - \mathbf{C} \hat{\mathbf{x}}_k) \\ &= (\mathbf{A} - \mathbf{L}\mathbf{C}) \mathbf{e}_k \end{aligned} \quad (14)$$

The dynamic behavior of the state estimation error \mathbf{e}_{k+1} at $t_{k+1} = (k+1)\Delta t$ is determined by $\mathbf{A} - \mathbf{L}\mathbf{C}$ and depends on the preceding error \mathbf{e}_k . Thus, in general, the model based grid voltage estimator is an Infinite Impulse Response (IIR) filter. This is fundamentally different from the Fourier series based methods, which are essentially FIR filters.

If $\mathbf{L} = 0$, \mathbf{e}_k tends to zero if all eigenvalues of \mathbf{A} lie within the unit circle. \mathbf{A} being a rotation matrix, its eigenvalues lie exactly on the unit circle, and without some feedback, it is impossible to reduce the state estimation error.

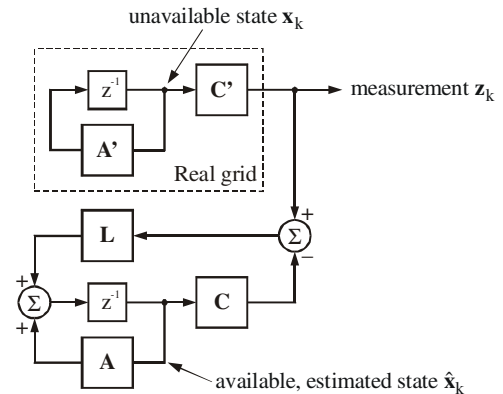


Fig. 2. Model based grid voltage estimation.

Using pole placement techniques to determine $\mathbf{L} \neq 0$, the eigenvalues of $\mathbf{A} - \mathbf{L}\mathbf{C}$ can be moved towards the center of the unit circle, leading to a (faster) decay of \mathbf{e}_k , assuming that the system is controllable. It is generally known (e.g. [9]) that \mathbf{e}_k in Fig. 2 is controllable if:

$$\text{Rank}[(\mathbf{A}^T)^{n-1}\mathbf{C}, \dots, \mathbf{A}^T\mathbf{C}, \mathbf{C}] = n \quad (15)$$

with n the number of states in the system or the number of elements in \mathbf{e}_k . Since \mathbf{A} is a rotation matrix, this condition is usually fulfilled unless n is so large that the $(\mathbf{A}^T)^{n-1}$ start to overlap.

\mathbf{L} can be chosen in such way that $\mathbf{e}_k = 0$ in at most n cycles, leading to a deadbeat response. In that case however, the sensitivity is high to process and measurement noises, $\mathbf{w}(t)$ and $\mathbf{v}(t)$, which have a detrimental effect on the estimation. By moving the system poles away from zero, one obtains a reduced sensitivity to $\mathbf{w}(t)$ and $\mathbf{v}(t)$ at the expense of an increased settling time. If $\mathbf{w}(t)$ and $\mathbf{v}(t)$ are white and a Minimal Squared Estimation Error (MSEE) is desired, the Kalman filter provides an optimum for \mathbf{L} , usually referred to as \mathbf{K} .

G. Model errors and \mathbf{Q}

A remark concerning the modeling error is in place here. In many cases, $\mathbf{w}(t)$ or its spectrum is not well known. Sometimes, the errors are systematic and cannot be represented by a white noise sequence.

If the noise is still stochastic but non-white, the system model can be extended to include a filter in order to generate a colored noise signal, on which the model can depend subsequently. This technique is called ‘state augmentation’.

In some cases, the real system contains even an unknown deterministic input. For example, consider the ‘process’ of the sinusoidal grid voltage. An unknown ‘load signal’ at its unavailable ‘input’ varies the output voltage and phase. While monitoring this process, one often considers the unknown input signal as a noise contribution and includes it in the \mathbf{Q}_k matrix. This is a questionable practice as the load signal is probably non-white, i.e. loads are usually switched on or off for an extended period. During transitions, the Kalman gain is no longer an optimum blending factor in the MSEE sense, but the estimator response may still be acceptable in practice .

Methods exist to determine \mathbf{Q}_k during Kalman filter operation and the papers of [10] and [11] may provide a useful starting point for the interested reader.

H. Computational effort

In the case that multiple harmonic frequencies are introduced in the model, \mathbf{A}_{OSC1} becomes semi-diagonal and the computational effort is $(2+k)N$, k indicating the number of measurements i.e. number of rows in \mathbf{C}_{OSC1} . A frame containing N data samples therefore requires $(2+k)N^2$ operations, being slightly less than the FFT.

V. WAVELET BASED MEASUREMENT TECHNIQUES

The use of wavelets [12] introduces a totally different approach to the problem of determining phasors. They offer a trade-off between frequency and time resolution, something

the DFT is incapable of. An introduction to the application of wavelets in power analysis can be found in [13] and [15]. [14] discusses the wavelet transform as a harmonic analysis tool in general.

VI. ACKNOWLEDGMENTS

The authors are grateful to the Belgian ‘Fonds voor Wetenschappelijk Onderzoek Vlaanderen’ for its financial support of this work and the Research Council of the K.U.Leuven for granting a concerted research action to support this research. J. Driesen holds a postdoctoral research fellowship of the Belgian ‘Fonds voor Wetenschappelijk Onderzoek – Vlaanderen’.

VII. REFERENCES

- [1] Robinson I. A., ‘An optical-fibre ring interface bus for precise electrical measurements,’ *Measurements Science Technology*, No. 2, pp. 949-956, 1991.
- [2] Texas Instruments Inc., ‘THS5500 14 bit 125MSPS Analog-to-Digital Converter,’ *Data sheet, Document No. SBAS303C, Revd. 2004*, March 2004.
- [3] Papoulis A., ‘The Fourier Integral and its applications,’ *McGraw-Hill*, New York, 1962.
- [4] Bergland G. D., ‘A Guided Tour of the Fast Fourier Transform,’ *IEEE Spectrum*, Vol. 6, pp. 41-52, July 1969.
- [5] Van den Keybus J., ‘Development of a Universal Electric Energy Measurement and Control Platform for Low-Voltage Grid-Coupled Applications in a Deregulated Electricity Market,’ *PhD Dissertation, K.U.Leuven*, Leuven, pp. 39-41, December 2003.
- [6] Brown R. G., Hwang Y. C., ‘Introduction to Random Signal Analysis and Applied Kalman Filtering,’ *John Wiley & Sons*, New York, 1985.
- [7] Girgis A., Bin Chang W., Makram E. B., ‘A Digital Recursive Measurement Scheme for On-Line Tracking of Power System Harmonics,’ *Trans. IEEE Power Delivery*, Vol. 6, No. 3, pp. 1153-1159, July 1991.
- [8] Sachdev M. S., Nagpal M., ‘A Recursive Least Error Squares Algorithm for Power System Relaying and Measurement Applications,’ *Trans. IEEE Power Delivery*, Vol. 6, No. 3, pp. 1008-1015, July 1991.
- [9] Meyr H., ‘Regelungstechnik und Systemtheorie,’ 2. *Heft*, Lehrstuhl für Elektrische Regelungstechnik, Rheinisch-Westfälische Technische Hochschule (RWTH), Aachen, Germany, 1991.
- [10] Mehra R. K., ‘On the Identification of Variances and Adaptive Kalman Filtering,’ *Trans. IEEE Automatic Control*, Vol. 15, No. 2, pp. 175-184, April 1970.
- [11] Carew B., Bélanger P. B., ‘Identification of Optimum Filter Steady-State Gain for Systems with Unknown Noise Covariances,’ *Trans. IEEE Automatic Control*, Vol. 18, No. 6, pp. 582-587, December 1973.
- [12] Mallat S., ‘A Wavelet Tour of Signal Processing,’ *Academic Press*, San Diego, 1999.
- [13] Yoon W.-K., Devaney M. J., ‘Power Measurement Using the Wavelet Transform,’ *Trans. IEEE Instrumentation. and Measurement*, Vol. 47, No. 5, pp. 1205-1210, 1998.
- [14] Newland D. E., ‘Harmonic wavelet analysis,’ *Proc. R. Soc.*, London, A443, pp. 203-225, 1993.
- [15] Driesen J., Belmans R., ‘Wavelet-based power quantification approaches,’ *IEEE Transactions on Instrumentation and Measurement*, vol. 52, no. 4, August, 2003; pp. 1232-1238.